Bulletin of the JSME, Vol. 21, No. 155, May, 1978



621.914.5:621.833

Paper No. 155 −18

# Numerical Analysis of Hobbing in Unfinished Space*

By Kenichi TERASHIMA** and Taku UENO***

The hobbing theory of generating the involute gear teeth has been often reported. However, a hobbing mechanism of enlarging the unfinished tooth space has been rarely investigated, because this mechanism is very complicated and the cutting behaviors are different with each tooth and even in the position on one tooth profile.

In order to make clear the causes of the tooth wear and the hobbing vibration, it is necessary to know the cutting behaviors at any point on the edge. This paper describes a method of calculating the length and the thickness to be cut on each point closely divided along the tooth profile without neglecting the tip roundness.

This method can be applied to any hobbing condition, e.g. to the cases of spur or helical gear, and the conventional or the climb hobbing. Some examples analyzed by this method are compared with the practical hobbing results, and then some suggestions for both wear and vibration analyses are given.

## 1. Introduction

Rapid wearing of hob teeth is not desirable from the viewpoint of the gear accuracy, the machining efficiency and the higher price of tool. The wears of hob teeth are influenced by many factors such as materials, heat treatment, hardness, shapes and dimensions of the tool and the gear, and speed, feed and direction in the cutting, and the cutting oil and vibration during the hobbing.

In order to investigate quantitatively and synthetically the influence of such factors, it is necessary to grasp the cutting thickness and length at any position along the tooth profile. But the hobbing mechanism is very complicated, because the cutting behaviors are different in every tooth and at the position along tooth profile even in one tooth. The hobbing mechanism in the unfinished tooth space of gear has been analyzed on the cutting of the top edge and the side ones respectively, and the tip roundness has been neglected in spite of its importance,[1]~[3] but a large wear generally appears at the flank of this roundness.

The present paper describes a method of calculating strictly the entering angle, the cutting thickness and length in every revolution angle of hob without neglecting the round edge. This method can be applied to the analysis of cutting behavior of the hob teeth modified for anti-wear purpose, and also to the analysis of the cutting torque variation affecting the wear and chipping.

* Received 17th March, 1976.

** Professor, Faculty of Engineering, Nagasaki University, Nagasaki City.

*** Professor, Faculty of Engineering, Kyushu University.

## 2. Analysis of cutting mechanism in unfinished tooth space

The hobbing in unfinished tooth space removes a part of curved space surface with each tooth of hob. This space hobbing can be analyzed through the state of many imaginary normal segments standing in the space, because the segments are shortened with every tooth.

In this paper, the analysis is made under such a condition that the right hand helical gear (module $m_n$, pressure angle $\alpha_c$ number of teeth $Z_p$ and helix angle $\beta$) is cut conventionally by feed $f_t$ with the same hand helix hob (outside radius $r_k$, number of threads $Z_w$, straight gashes, gash number $G_n$, rake angle $0°$).

$\beta$ becomes minus for left hand helical gear, $\beta = 0°$ for spur gear, and $f_t < 0$ for climb hobbing. When the left hand helix hob is used, a drawing view designed for right helix hob is symmetrically reversed from right to left. The conditions necessary to analyze, and the equations to calculate the dimensions of gear and hob which are decided through given data are listed in Table 1.

### 2.1 Hobbing mechanism

Figure 1 illustrates the right hand helical gear being hobbed with the same hand hob. The hobbing mechanism fixing the gear revolution can be considered a helical motion of the hob which revolves around the fixed gear, in spinning about the hob axis and in leading parallel to the gear axis by feed. In this case, Eq.(1) relates with the spinning angle $\theta$, the revolving angle $\Theta$ and the lead $f$ through the formula of the relative revolution given for both the hob and the gear.

$$\Theta = K_1\theta, \quad K_1 = (Z_w/Z_p)/\{1-f_t\sin\beta/(\pi m_n Z_p)\}$$
$$f = K_2\Theta, \quad K_2 = f_t/(2\pi) \qquad \cdots\cdots\cdots(1)$$

The positive or negative signs of $\theta$, $\Theta$, $\beta$, $f$ and other symbols used in this paper are

shown in Table 2.

Figure 2 illustrates the co-ordinate systems, in which a* shows the state of a tooth cutting most deeply into the gear blank. This position is named the generating center of hobbing. At this time, the center line of hob tooth profile coincides with the one of gear tooth space, and these center lines also coincide respectively with a common normal line $Y_g$ of hob and gear axes.

Here, a gear co-ordinate system $X_g\ Y_g\ Z_g$ having the gear axis as $Z_g$ and the common normal as $Y_g$ is fixed in the gear. A tooth space co-ordinate system $X_s\ Y_s\ Z_s$ has $Y_g$ axis as $Y_s$ and a line tangent to a center line of the tooth space as $Z_s$, and this system exists in the tooth space. The gear system is related to the space system by the following equations.

$$X_g = X_s\cos\beta - Z_s\sin\beta, \quad Y_g = Y_s, \quad Z_g = X_s\sin\beta + Z_s\cos\beta \qquad \cdots\cdots(2)$$

In a hob co-ordinate system $X_h\ Y_h\ Z_h$, $X_h$ is the hob axis at a position where the hob revolves helically by angle $\Theta$ from $O_h$ to $O_h'$, and $Y_h$ is a common normal line between gear axis $Z_g$ and $X_h$ axis. Because this system moves helically about $Z_g$ axis with the relation described by Eq.(1), a relation shown by Eq.(3) holds for both the hob and the gear system.

$$X_h = (X_g\cos\Theta - Y_g\sin\Theta)\cos\Gamma + Z_g + f$$
$$Y_h = cd - (X_g\sin\Theta + Y_g\cos\Theta) \qquad \cdots\cdots(3)$$
$$Z_h = -(X_g\cos\Theta - Y_g\sin\Theta)\sin\Gamma + Z_g + f$$

Where $\Gamma$: setting angle of hob, $f$: feed [Eq.(1)], $cd$: center distance between gear and hob.

In the state of tooth $b'$ located at distance $X_n$ from $O_h'$ on the hob axis cutting down by angle $\theta_h$ in the space, a tooth profile co-ordinate system $X_c\ Y_c$ is decided, that is, $X_c$ is the hob axis and $Y_c$ is a center line of tooth profile. This is a plane co-ordinate and rotates around the hob axis $X_h$ with the hob spin.

## 2.2 Tooth number and profile division number

As shown in Fig.3, co-ordinate $X_{bj}\ Y_{bj}$ at boundaries $j = 1,2,3,\cdots 6$ can be decided for the tooth profile consisting of straight line $\overline{12}, \overline{34}, \overline{56}$ and circular arc $\widehat{23}\ \widehat{45}$. These calculating formulas are shown in Table 3(a).

In order to know the cutting amount at any position along the tooth profile, the whole profile is subdivided and the co-ordinates at each profile division are calculated respectively. In an example of chapter 3, interval $\overline{16}$ is divided into 50 equal lengths, and intersections of tooth profile and normal line at each interval division $i'$ are chosen as the profile divisions, and then all profile divisions are

Table 1 (a) Data to be given

| | | |
|---|---|---|
| Common | Module<br>Pressure angle | $m_n$<br>$\alpha_c$ |
| Gear | Number of teeth<br>Helix angle | $Z_p$<br>$\beta$ |
| Hob | Outside diameter<br>Tip round radius<br>Number of gashes<br>Number of threads<br>Helix hand | $r_k$<br>$r_t$<br>$G_n$<br>$Z_w$<br>Right |
| Cutting | Feed / Table rev.<br>-:climb, +:conven. | $f_t$<br>$\pm f_t$ |

Table 1 (b) Dimensions of gear and hob

| | |
|---|---|
| Gear | $R_0 = Z_p\ m_n / (2\cos\beta)$<br>$R_k = R_0 + m_n$<br>$R_r = R_0 - 1.25\ m_n$<br>$R_g = R_0\ \cos\{\tan^{-1}(\tan\alpha_c/\cos\beta)\}$ |
| Hob | $r_0 = r_k - 1.25\ m_n$<br>$r_d = r_0 - m_n$<br>$m_a = m_n / \cos\gamma$<br>$\gamma = \sin^{-1}\{\pi\ m_n Z_w/(2\pi r_0)\}$ |

(Standard tooth form)

Table 2 Plus or minus of used symbols

| Items | Symbols | Plus or minus |
|---|---|---|
| Tooth number | $N\ N_0\ N_r$ | Preceding tooth side : + |
| Tooth position | $X_n\ X_0\ X_r$ | Preceding tooth side : + |
| Spinning angle | $\theta\ \theta_n\ \theta_h$ | Cutting rev.-wise : - |
| Revolut. angle | $\Theta\ \Theta_p\ \Theta'\Theta''$ | Clockwise in Fig.2 : + |
| Feed of hob | $f_t\ f_h\ f'_f$ | Climb: -, Conventional: + |
| Helix angle | $\beta$ | Right helix hand : + |
| Setting angle | $\Gamma$ | According to ± of $(\beta - \gamma)$ |
| Lead angle | $\gamma$ | Right helix hand : + |
| Co-ordinate | $X\ Y\ Z$ | Arrow direction(Fig2): + |

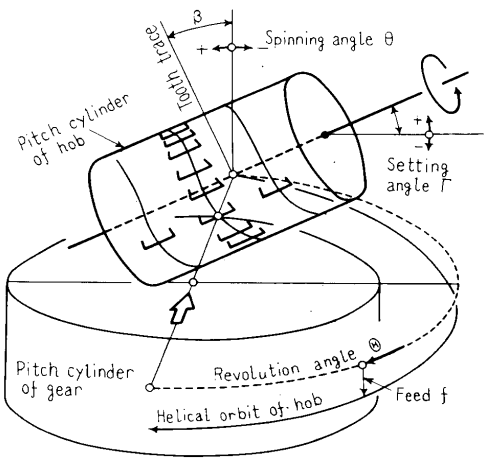


Fig.1 Hobbing mechanism

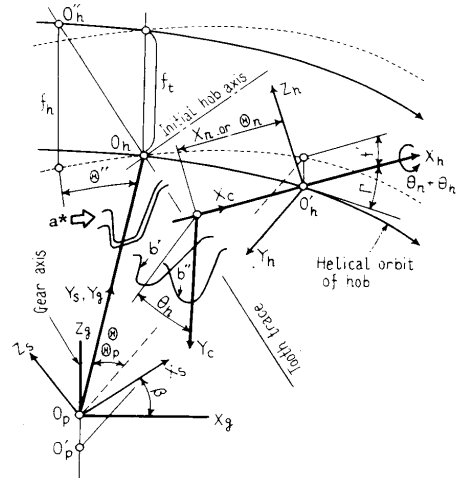


Fig.2 Co-ordinate systems

numberd in turn as $X_{ci}$ $Y_{ci}$, which can be calculated by formulas shown in Table 3(b).

On the peripherally tapered or the profile modified hob, the positions of the boundaries and the profile divisions are different in every tooth. The raked hob is not a bisymmetry with respect to the center line of tooth form.

As shown in Fig.4, the generating center tooth a* of Fig.2 is named the *0*-tooth, and according to the order of preceging or succeeding from the *0*-tooth, each tooth is numbered as *1*-tooth, *2*-,*3*-,$\cdots$ or -*1*-tooth,-*2*-,-*3*-,$\cdots$. An axial distance $X_n$ and an angular position $\theta_n$ of the *N*-tooth are as follows,

$$X_n = \{\pi m_n Z_w/(G_n \cos\gamma)\}N$$
$$\theta_n = (2\pi/G_n)N, \quad \gamma : \text{lead angle of hob} \qquad \cdots\cdots\cdots(4)$$

When the hob spins about its axis by angle $\theta_n$ from the state a* (Fig.2), the *N*-tooth falls into a state $b'$ in which this tooth cuts most deeply into the gear blank. At a state $b''$ of the *N*-tooth after the hob spins by angle $\theta_n$ further, the revolution angle $\Theta_p$ and feed $f'$ of the hob are expressed from Eq.(1) as follows.

$$\Theta_p = K_1(\theta_n+\theta_h),\ f' = K_2\Theta_p,\ K_1,K_2 \text{ ; Eq.(1)} \qquad \cdots\cdots\cdots(5)$$

Table 3 (a) Profile boundaries

| Boundary | | $Xbj$ | $Ybj$ | Constants |
|---|---|---|---|---|
| $j$ = 1 | | $m_n(0.25\pi+\tan\alpha_c)/\cos\gamma$ | $r_0-m_n$ | $rt = 0.375\ m_n$ |
| 2 | | $(E+D)/\cos\gamma$ | $rk-B$ | $A = 1.25\ m_n-B$ |
| 3 | | $E/\cos\gamma$ | $rk$ | $B=rt(1-\sin\alpha_c)$ |
| 4 | | $-Xb_3$ | $Yb_3$ | $C = A\tan\alpha_c$ |
| 5 | | $-Xb_2$ | $Yb_2$ | $D = rt\cos\alpha_c$ |
| 6 | | $-Xb_1$ | $Yb_1$ | $E = 0.25\pi\ m_n - C - D$ |
| Center of tip round | 7 | $Xb_3$ | $Y_0+G$ | $G=1.25\ m_n-rt$ |
| | 8 | $-Xb_7$ | $Yb_7$ | |

Table 3 (b) Profile divisions

| Between | $Yci$ are found from $Xci$ |
|---|---|
| $j$ 1 ~ 2 | $2m_n(Xb_1-Xci)/(Xb_1-Xb_2)+rd$ |
| 2 ~ 3 | $\{rt^2-(Xci-Xb_7)^2\}^{0.5}+Yb_7$ |
| 3 ~ 4 | $rk$, $rt$ : Tip round radius |
| 4 ~ 5 | $\{rt^2-(Xci-Xb_8)^2\}^{0.5}+Yb_8$ |
| 5 ~ 6 | $2m_n(Xb_6-Xci)/(Xb_6-Xb_5)+rd$ |
| Equal division | $\Delta Xc = \dfrac{2(0.25\pi+\tan\alpha_c)m_n}{n\cos\gamma}$ |

$n$ : Equally divided numbers

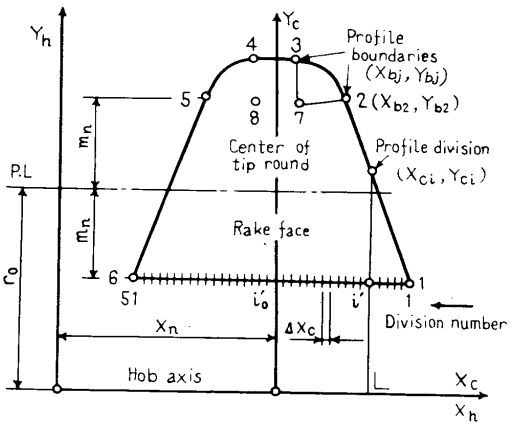


Fig.3 Boundaries and divisions of the tooth profile

The relation between gear co-ordinate and hob one, in this case, can be described as follows through Eq.(3).

$$X_h = (X_g\cos\Theta_p - Y_g\sin\Theta_p)\cos\Gamma + Z_g + f'$$
$$Y_h = c_d - (X_g\sin\Theta_p + Y_g\cos\Theta_p)$$
$$Z_h = -(X_g\cos\Theta_p - Y_g\sin\Theta_p)\sin\Gamma + Z_g + f' \qquad \cdots\cdots\cdots(6)$$

Through Eq.(4), the relation of the *N*-tooth profile to the hob co-ordinate is shown as follows,

$$X_h = X_n + X_c,\quad Y_h = Y_c\cos\theta_h,\quad Z_h = Y_c\sin\theta_h \qquad \cdots\cdots\cdots(7)$$

## 2.3 Cutting zone preceding tooth

In the case that the upper or lower sign of ± or ∓ corresponds to the left or the right side edge respectively, an axial zone $X_0$ where the hob generates the involute tooth profile (Fig.5) and a tooth number $N_0$ at its zone end are described as follows through Fig.6.

$$X_0 = m_n(\cos^2\beta/\tan\alpha_c + \tan\alpha_c \pm 0.25\pi)/\cos\gamma$$
$$N_0 = X_0/\Delta t_a,\quad \Delta t_a = \pi m_n/(G_n\cos\gamma) \qquad \cdots\cdots\cdots(8)$$

$\Delta t_a$ : axial division pitch

Figure 7 is Fig.5 as viewed in the direction of a white arrow⇨, in which the lower end $U$ of the unfinished tooth space is tangent just to lower end face $e$ of the gear. With respect to $y$ $z$ co-ordinate, in which two axes are respectively parallel to $Y_h$ and $Z_h$ axes and run through the gear center, a peripheral circle $c$ of hob and a peripheral ellipse $e$ of gear end face are expressed as follows.

$$\text{Hob : } z_h = Z_r - \sqrt{r_k^2 - (c_d - y)^2}$$
$$\text{Gear: } z_g = \sqrt{R_k^2 - y^2}\sin\Gamma \qquad \cdots\cdots\cdots(9)$$

By finding a contact point $y_0$ $z_0$ of circle $c$ and ellipse $e$, a rough cutting range $X_r$ and its tooth number $N_r$ are given by

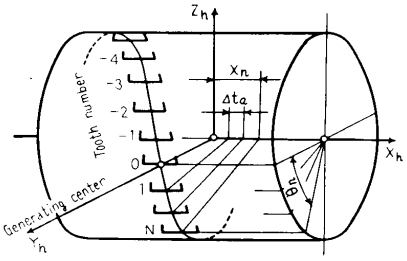


Fig.4 Tooth number $N$ and tooth position $X_n$ $\theta_n$

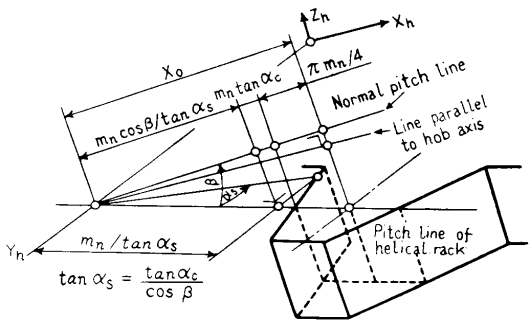


Fig.6 Involute generating zone $X_0$

$X_r = \bar{X}\cos\Gamma + Z_r\tan\Gamma$, $N_r = X_r/\Delta t_a$
$\bar{X} = \sqrt{Rk^2 - y_0^2}$, $Z_r = z_0 + Z_r'$, $\Delta t_a$ : Eq.(8)
$Z_r' = \sqrt{rk^2 - (c_d - y_0)^2}$
.....(10)

Figure 8 is a projection in a white arrow direction of Fig.1 and this shows a cutting zone in the tooth space. $N_0$-tooth begins the involute generation at its position $Oh_0$, $0$-th tooth is at the generation center of $Oh$, $-N_0$-tooth ends the involute generation at $Oh_0'$, and $-N_r$-tooth ends the rough cutting at $Oh_r$.

$Z_r'$ in Eq.(10) is a length cut down with $N_r$-tooth in the tooth space. In this period, the $N_r$-tooth rotates from cutting most deeply into the gear to coming out of the gear peripheral surface. The generating zone $Z_0$ and the rough cutting zone $Z_r$ in the tooth space direction are given as follows through Fig.8.

$Z_0 = \{X_0^2 + \overline{Oh_0Oh}^2 - 2X_0\overline{Oh_0Oh}\cos(\Gamma+\gamma')\}^{1/2}$
$Z_r = \{X_r^2 + \overline{Oh_0Oh_r}^2 - 2X_r\overline{Oh_0Oh_r}\cos(\Gamma+\gamma')\}^{1/2}$
$\gamma' = \tan^{-1}\{f_t/(2\pi R_0)\}$
$\gamma'$ : lead angle of helical orbit
$\overline{Oh_0Oh_0} = \sqrt{R_0^2 + K_2^2}\,\Theta_0$, $\Theta_0 = K_1(2\pi/G_n)N_0$
$\overline{Oh_0Oh_r} = \sqrt{R_0^2 + K_2^2}\,\Theta_r$, $\Theta_r = K_1(2\pi/G_n)N_r$
.....(11)

According to the helical hand of gear tooth and the direction of hob feed (depending on $\beta$ and $f_t$ being + or - according to Table 2), either $N_0$- or $N_r$-tooth begings cutting at first. $Z_0$ and $Z_r$ in Eq.(11), $Z_r'$ in Eq.(10) and the upper cutting zone $Z_u$ and the lower one $Z_d$ from generating center are shown in Fig.8.

## 2.4 Layer division and normal segment

A rectangular $ABCD$ in Fig.9 is a plane normal to the tooth space at the generating center. The whole cutting zone $Z_u + Z_d$ is divided into suitable equal intervals, and then the same rectangles at each division are named layer number $1,2,3,\cdots J\cdots$ from above. $\overline{T_1T_2}$ is a tooth space clearance on the outside diameter of gear and is divided into $n$ equal parts (e.g. $n=50$ in the later example) and further the line segments normal to $\overline{T_1T_2}$ at each division are numbered segment $1,2,3,\cdots K\cdots 51$ from left side as Fig.9. $J$-layer is at a position rotated by angle $\Theta'$ from $J_0$-layer (generating layer). Here,

$\Theta' = \{\Delta Z_g(J-J_0)\tan\beta\}/R_0$ .....(12)
$\Delta Z_g = 0.15m_n/\cos\beta \fallingdotseq 3\Delta X_c/\cos\beta$

where the suitable values of layer interval $\Delta Z_g$ must be given in Eq.(12). A segment interval $\Delta X_s$ is expressed as follows.

$\Delta X_s = 2R_{kv}\sin\{\phi(R_{kv})\}/n$
$\phi(R_{kv}) = 0.5\pi/Z_v + \mathrm{inv}\alpha_c - \mathrm{inv}\{\cos^{-1}(R_{gv}/R_{kv})\}$
$Z_v = Z_p/\cos^3\beta$, $R_{0v} = 0.5Z_vm_n$
$R_{kv} = R_{0v} + m_n$, $R_{gv} = R_{0v}\cos\alpha_c$
: equivalent spur gear of helical gear
.....(13)

$X_t'Y_t'Z_t'$ and $X_r'Y_r'Z_r'$ are the gear co-ordinates of top and root of $J$-layer $K$-segment, which are expressed as follows.

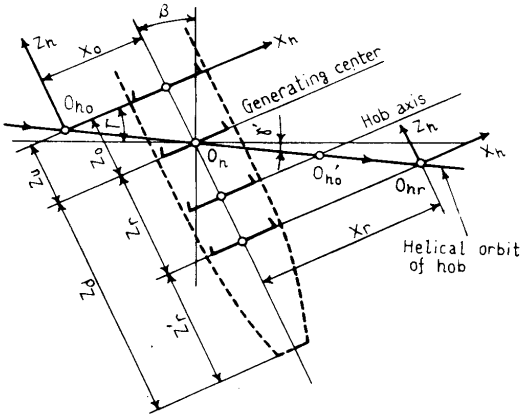


Fig.8 Cutting zone in the tooth space

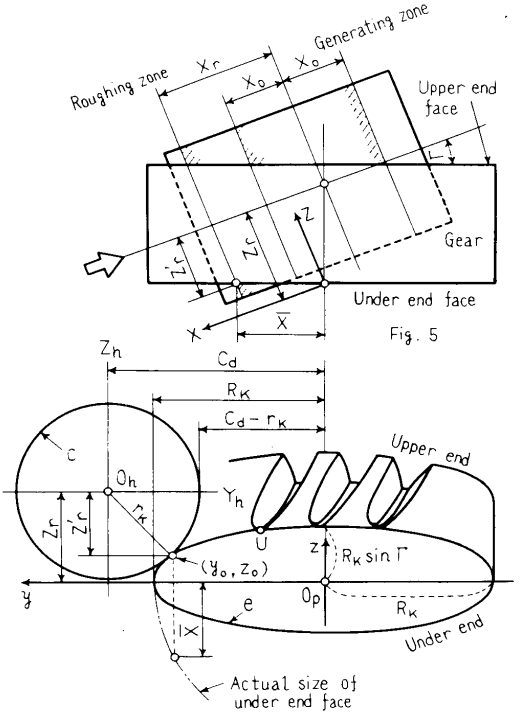


Fig.7 Roughing zone $X_r$ and cutting down length $Z_r'$

Figure 7 is obtained by looking Fig.5 in the hob axis direction.

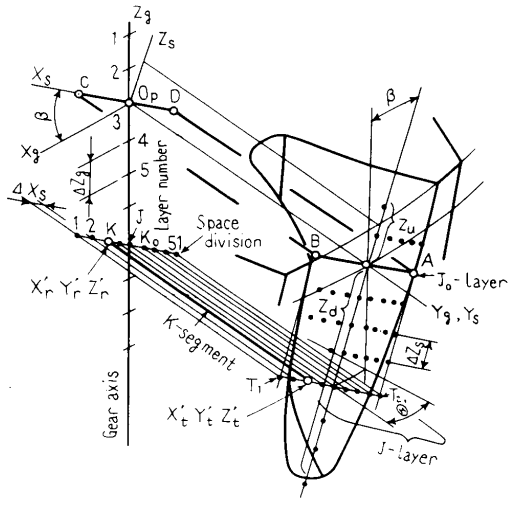


Fig.9 Layer $J$ and normal segment $K$ in the tooth space

$$X_r' = X_k\cos\Theta',\quad Y_r' = X_k\sin\Theta',\quad X_k = \Delta X_g(K-K_0),$$
$$Z_r' = \Delta X_s(K-K_0)\sin\beta + \Delta Z_g(J-J_0),$$
$$X_t' = X_k\cos\Theta' - Y_{jk}\sin\Theta',\quad \cdots(14)$$
$$Y_t' = X_k\sin\Theta' + Y_{jk}\cos\Theta',\quad Z_t' = Z_r'$$
$$Y_{jk} = \sqrt{R_k^2 - X_k^2},\quad \Delta Z_s = \Delta Z_g/\cos\beta$$

Thus, many line segments stand in rows in the tooth space and they are shortened by cutting with each hob tooth passing through the tooth space.

## 2.5 Shortening of line segment

Figure 10 shows a scene where the cutting edge of $N$-tooth meets just the $J$-layer $K$-segment. If the hob co-ordinate $X_i\,Y_i\,Z_i$ of their intersection is found, the cutting thickness $t_3$ can be calculated from a real length $\Delta t$ of $t_1$ to be cut away.

The process of calculating $X_iY_iZ_i$ is shown in Table 4. In accordance with the order shown in this Table, the values in right column can be obtained through the given data and the formulas in the center column. In order that $N$-tooth may intersect the objective segment $K$, the hob must be spun by angle $\theta_n+\theta_h$ from state a* to b" as shown in Fig.2, where $\theta_n$ is decided by the given tooth number through Eq.(4), but the cut down angle $\theta_h$ is unknown. Accordingly, after starting from an initial value given by order 4, $\theta_h$ must be increased in the accuracy through the calculation repeated from order 5 to 11.

Figure 10 shows a state of order 8, where Fig.(a) is a view of projecting both $J$-segment and $N$-tooth profile on the plane $X_hY_h$ after the hob spins by angle $\theta_h+\theta_{h_1}$. The gear co-ordinate $X_r'\,Y_r'\,Z_r'$ and $X_t'\,Y_t'\,Z_t'$ of segment root and tip are transformated to the hob co-ordinate $X_r\,Y_r\,Z_r$ and $X_t\,Y_t\,Z_t$ through Eq.(6).

$X_i\,Y_i$ are co-ordinates of an intersection of $K$-segment and $N$-profile, which can be obtained as the problem of plane geometry. The profiles $\widehat{23}$ and $\widehat{45}$ are one part of ellipse in which tip round circle is inclined by angle $\theta_h$. And further, if $Y_i$ is equal to or less than $Y_t$, the cutting edge dose not cut this segment, so that whether the segment is cut or not must be judged through order 9.

As shown in Fig.10(a), $Zi_1$ of order 10 is a hob co-ordinate $Z_h$ of $Y_i$ up to the tooth profile $l$ projected on the plane $Y_h\,Z_h$, and $Zi_2$ is $Z_h$ co-ordinate of $Y_i$ to the segment. When close agreement is obtained between $Zi_1$ and $Zi_2$, the tooth edge intersects with the segment. Therefore, the accuracy of $X_i\,Y_i\,Z_i$ is increased in changing the value $\theta_{h_1}$ until $|\theta_{h_1}-\theta_{h_2}|$ becomes a given allowable value and the calculation is respected from order 5 to 11. The real length $\Delta t$ of cut away thickness $t_1$ and the remaining length $Y_{jk}$ of segment are expressed as follows.

$$\Delta t = \{(X_t-X_i)^2+(Y_t-Y_i)^2+(Z_t-Z_i)^2\}^{1/2}$$
$$Y_{jk} = \{Y_{jk}\text{ of Eq.(14)}\}-\Delta t \quad \cdots\cdots\cdots(15)$$

Since the line segment is cut away by $\Delta t$ with the $N$-tooth, in the calculation of next $(N-1)$-tooth, the left side $Y_{jk}$ of the above equation must be used as the length of $J$-layer $K$-segment, and $X_t\,Y_t\,Z_t$ of the top co-ordinate must be substituted by $X_i\,Y_i\,Z_i$.

## 2.6 Cutting thickness, width and length

The cut away length $\Delta t$ of segment is generally small, so that $t_2$ [Fig.10(b)] which is $\Delta t$ projected on the rake face is obtained, and its component $t_3$ normal to the tooth profile can be considered the thickness to be cut away from gear tooth face. $X_i'\,Y_i'$ is $X_i\,Y_i$ rotated from rake face $l$ to $l'$[Fig.10(a)], and $t_3$ can be calculated as follows through Figs.10 and 3.

$$X_i' = X_i,\quad Y_i' = Y_i/\cos\theta_h$$
$$Y_t' = Y_t\cos\theta_h + Z_t\sin\theta_h$$
$$\overline{34}\quad : t_3 = Y_i' - Y_t'$$
$$\overline{12},\ \overline{56}\quad : t_3 = t_2\sin[\alpha_c + \tan^{-1}\{(X_i-X_t)/(Y_i'-Y_t')\}]$$
$$\widehat{23},\ \widehat{45}\quad : t_3 = t_2\cos\{(X^2+t_2^2-Y^2)/(2Xt_2)\}$$
$$t_2 = \{(Y_i'-Y_t)^2+(X_i-X_t)^2\}^{1/2}$$
$$\widehat{23}\quad : X^2 = (X_i'-X_{b7})^2+(Y_i'-Y_{b7})^2$$
$$Y^2 = (X_t-X_{b7})^2+(Y_t'-Y_{b7})^2$$
$$\widehat{45}\quad : X^2 = (X_i'-X_{b8})^2+(Y_i'-Y_{b8})^2$$
$$Y^2 = (X_t-X_{b8})^2+(Y_t'-Y_{b8})^2 \quad \cdots\cdots\cdots(16)$$

Table 4 Precedure of finding intersection $XiYiZi$

| Order | Data to be given | Eq. | Values to be found |
|---|---|---|---|
| 1 | Tooth number $N$ | Eq.(4) | Nth position $X_n\ \Theta_n$ |
| 2 | Segment number $J,K$ | Eq.(14) | $Xt'Yt'Zt', Xr'Yr'Zr'$ |
| 3 | Segment tip $Xt'Yt'Zt'$ | Eq.(6) | Hob co-ord. $XtYtZt$ |
| 4 | Tip co-ordinate $Yt\ Zt$ | | St. $\theta_h=\tan^{-1}(Zt/Yt)$ |
| 5 | Spinning angle $\Theta_n\ \Theta_h$ | Eq.(5) | Rev.ang.$\Theta_p$, feed $f'$ |
| 6 | $Xt'Yt'Zt', Xr'Yr'Zr'$ $\Theta_p$ and $f'$ | Eq.(6) | $XtYtZt, XrYrZr$ in hob co-ordinate |
| 7 | Profile boundaries | Eq.(7) | $XbjYbjZbj,\ j=1\ \ 6$ in hob co-ordinate |
| 8 | $Xb_1Yb_1,\cdots Xb_6Yb_6$ and $XtYt,\ XrYr$ | Fig.10 | Intersection $XiYi$ |
| 9 | $Yi \leqq Yt$ : No cutting | ⟶ | $K = K = 1$, GO TO 2 |
| | $Yi > Yt$ : Cutting | ↘ | After find. $Zi_1\,Zi_2$ |
| 10 | $Yb_1Zb_1,\cdots,Yb_6Zb_6$ | | $\theta_{h_1}=\tan^{-1}(Zi_1/Yi)$ |
| | $YtZt,\ YrZr,\ Yi$ | ⟶ | $\theta_{h_2}=\tan^{-1}(Zi_2/Yi)$ |
| 11 | $\lvert\theta_{h_1}-\theta_{h_2}\rvert >$ Allowable | ⟶ | $\theta_h=\theta_{h_2}$, GO TO 5 |
| | $\lvert\theta_{h_1}-\theta_{h_2}\rvert \leqq$ value | ⟶ | $\theta_h=\theta_{h_2}, XiYi, Zi=Zi_2$ |

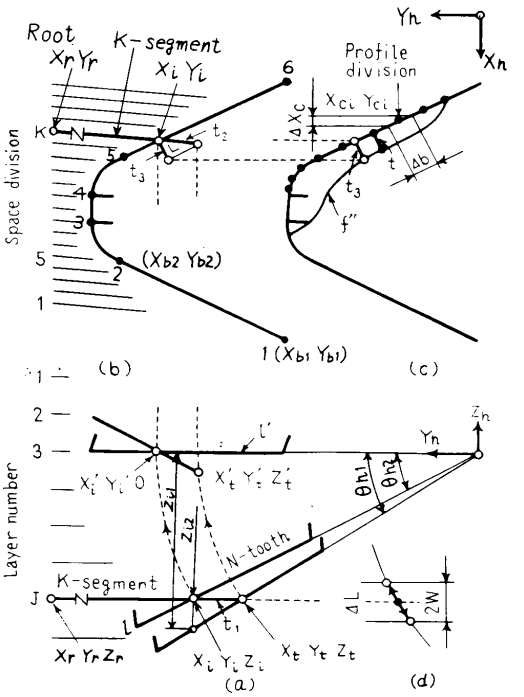


Fig.10 Intersection $XiYi$ of $N$-tooth and $K$-segment, and cutting thickness, width and length

In this way, if the cutting thickness $t_3$ is calculated for each segment on one layer, a section $f''$ [Fig.10(c)] to be cut away on the this layer when the hob tooth passes through this layer can be drawn on the rake face. Cutting thickness $t$ at each profile division is obtained by interpolating with respect to $f''$-curve.

As shown in Fig.(c), when the tooth edge at the profile division $X_{ci}$ $Y_{ci}$ does cutting, the following $\Delta b$ gives a cutting width at its division.

$\Delta b = \Delta X_c / \sin\eta$, $\Delta X_c$ : Table 3(b)

$\overline{34}$ : $\eta = 0.5\pi$

$\overline{23}$ : $\eta = \tan^{-1}\{(Y_{ci}-Y_{b7})/(X_{b7}-X_{ci})\}$

$\overline{45}$ : $\eta = \tan^{-1}\{(Y_{ci}-Y_{b8})/(X_{b8}-X_{ci})\}$

$\overline{12}$, $\overline{56}$ : $\eta = \alpha_c$

.....(17)

When the edge at $X_{ci}$ $Y_{ci}$ cuts the $K$-segment of $J$-layer, the cutting length $\Delta L$ is described as follows from Fig.(d).

$\Delta L = Y_{ci}[\sin^{-1}\{(Z_i+W)/Y_{ci}\} - \sin^{-1}\{(Z_i-W)/Y_{ci}\}]$

$W = 0.5\Delta Z_g \cos\Gamma$, $\Delta Z_g$ : Eq.(12)

.....(18)

Because $\Delta b$ and $\Delta L$ are different with the $X_{ci}$ $Y_{ci}$ position and with the layer position $Z_i$, it is convenient to prepare a chart. The hob tooth cuts downward from upper layer, therefore this calculation must be begun from segment $K=1$ of the upper layer $J=1$. After calculating all segments of one layer, the cutting thickness $t$ at each profile division is calculated by the interpolation, and then the same calculations are advanced toward the lower layers.

The tooth space form unfinished before one revolution of gear can be expressed by $Y_{jk}$ which is the segment length remaining after all teeth $N_0+N_r$ of the hob existing at $O_h''$(Fig.2) have passed through the gear tooth space. Position $O_h''$ is found from Eq.(1).

$f_h = f_t/\{1-f_t\sin\beta/(\pi m_n Z_p)\}$ .....(19)

$\Theta'' = f_h \tan\beta / R_0$

After finishing all calculations, a tooth profile drawn by plotting $Y_{jk}$ on the $J_0$-layer (generating plane) by interval $\Delta X_s$ [Eq.(13)] shows the involute to be finished at last. Therefore, in order to find the calculation error, this checking must be practiced. In a hob shortened in its length like one or two wound roughing one, the calculation must be made from Eq.(11) by using the tooth numbers at shortened position instead of $N_0$ and $N_r$.

## 3. Examples of calculation, experimentation and application

In a case that module 3 spur gear is conventionally cut with the hob having the outside radius 40 $mm$ under the feed 1.78 $mm$ where the details are listed in Table 5, an example of calculating the 16-tooth is

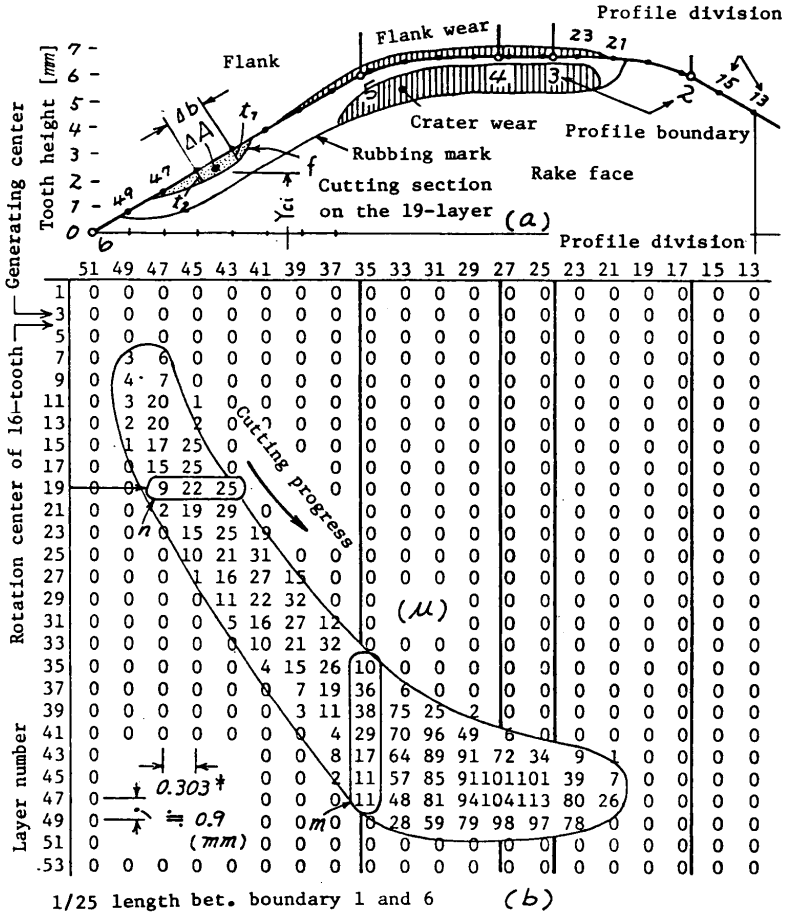


Fig.11 Hobbing by 16th tooth in unfinished tooth space

shown in Fig.11. In Figure(a), in order to see simultaneously the flank face, the rake face is tilted to this side. Numbers 1····51 on the abscissa correspond to the profile division black-marked along the tooth profile. Numbers 1,3,····53 on the ordinate are the layer numbers. Their intervals are 0.1515 and about 0.45 *mm* respectively.

The calculated results of cutting zone are shown in Table 6. When the tooth in Fig.(a) rotates downward and to this side and passes through each layer from upward, every progression arranged horizontally to right side of layer numbers shows the cutting thickness $t$ ($\mu m$) at each profile division. *0* zone expresses the non-cutting one and figure zone shows the cutting one.

The cutting progresses in the direction of thick arrow and this cutting begins from profile division 49 at left root and finishes at division 21 of top edge through tip round edge in moving along the tooth profile. Large corner wear grows frequently near boundary 5 corresponding to division 35.

Looking vertically the figure $m$ of division 35, this cutting does from layer 35 to 47 and then cutting thickness varies through 0 10 36 ··· 11 0 $\mu m$. In this way, the wear of tooth edge can be compared quantitatively with the cutting amounts, and the entering angle at each division also can be calculated by the figure train $m$.

When passing through *19*-layer, this tooth cuts on the division interval 43 ~ 47, because the figure train $n$ in a horizontal direction of *19*-layer indicates it. This section $f$ is figured on the left root of Fig.(a). Small area $\Delta A$ along the edge and the radius from hob axis to $\Delta A$ can be calculated by $Y_{ci}$ in Table 3(b), so that the cutting force $P$ and the torque $T$ acting on all sections can be found by Eq.(20).

From the cutting width $\Delta b$ [Eq.(17)] between the adjacent profile divisions and from the cutting thickness $t_1$ and $t_2$ at these divisions,

$$\Delta A = 0.5(t_1+t_2)\Delta b : \text{trapezoid} \qquad \cdots\cdots(20)$$
$$P = \Sigma(p_s \Delta A), \quad T = \Sigma(p_s \Delta A Y_{ci})$$

where $P_s$ is the specific cutting resistance. The fluctuations of cutting force $P$ and torque $T$ can be estimated theoretically through these calculations. The fluctuation per hob revolution must be considered synthetically that two teeth act simultaneously in the same tooth space and four or six teeth work in the adjacent tooth spaces at the same time.

Figure 11 is an example of *16*-tooth,

Table 5 Cutting condition

| | | | |
|---|---|---|---|
| Common | Module | $m_n$ | 3 *mm* |
| | Pressure angle | $\alpha_c$ | 20° |
| Gear | Number of teeth | $Z_p$ | 42 |
| | Tooth width | $b$ | 40 *mm* |
| | Helix angle | $\beta$ | 0° |
| Hob | Outside radius | $r_k$ | 40 *mm* |
| | Tip round radius | $r_t$ | 1.13 |
| | Number of gashes | $G_n$ | 12 |
| | Number of thread | $Z_w$ | RH 1 |
| Cutting | Feed / Table rev | $f_t$ | 1.78 |
| | Direction | | Conv. |
| | Speed *m/min* | $v$ | 51 |
| Blank | Materials | | SCM 3 |
| | Number of pieces | | 10 |

Table 6 Cutting zones

| | | | |
|---|---|---|---|
| Hob | Generating end | $N_0$ | ±10th tooth |
| | Roughing end | $N_r$ | 24th tooth |
| | Most preceding tooth | | +24th tooth |
| | Division distance | $\Delta X_c$ | 0.1515 *mm* |
| Tooth space | Generating zone | $Z_u$ | 1.35 *mm* |
| | Roughing zone | $Z_d$ | 22.95 *mm* |
| | Layer distance | $\Delta Z_g$ | ≒0.45 *mm* |

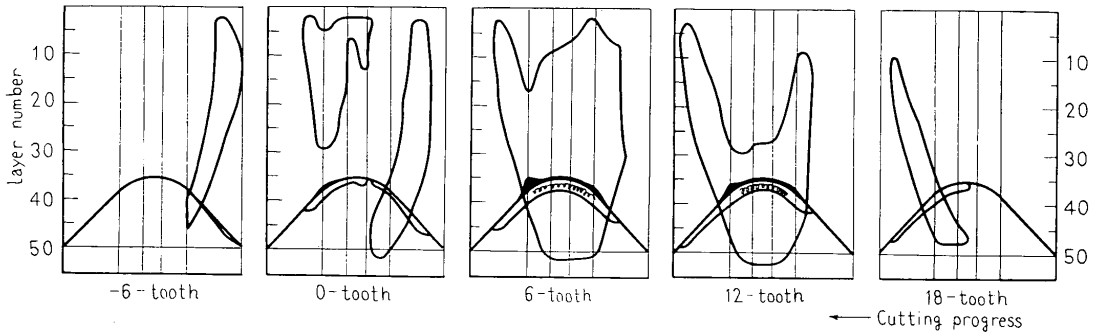


Fig.12 Calculated cutting zones in the tooth space

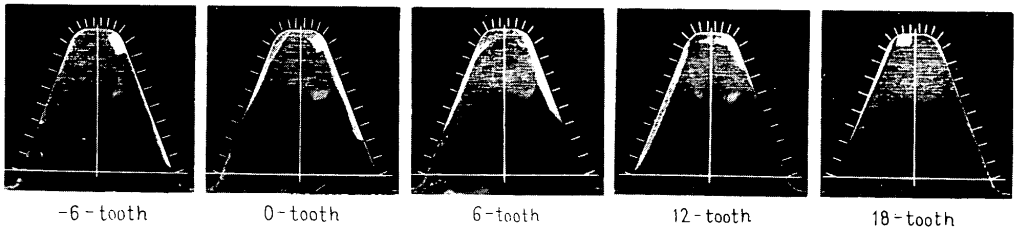


(Spur gear $m$ 3, $Z$ 42; Hob $r_k$ 40, single thread, 12 gashes; $f$ 1.78, conventional)

Fig.13 Measured cutting zone on the rake face

and the cases of other teeth are shown in Fig.12 where the ordinate scale is reduced to 1/3 for the abscissa. In this hobbing, one tooth space is cut with 34 hob teeth per gear revolution and 40 different chips are produced. Because the cutting section [$f$ in Fig.11(a)] on the rake face changes with the hob revolution, its measurement is difficult, so that 10 gears (SCM3, Hв190) were practically hobbed under the cutting speed 51 $m/min$ detailed in Table 5.

An example of comparing the rubbing marks on the rake face with the calculated cutting zone is shown in Figs.12 and 13, where the rubbing marks almost agree with the calculated ones. As the tooth wear can be related to the cutting amount, both the analyses of wear mechanism and the effects of factors influencing the wear can be considered quantitatively.

Figure 14 shows the cutting torque per hob revolution calculated through Eq.(20) under $m_n$ 4, $Z_p$ 33, β 0°, $r_k$ 50, $G_n$ 11, $Z_w$ 1, $f_t$ 2, climb (see the symbols in Table 5). Because the cutting section and its thickness vary every moment in the hobbing and suitable data of specific cutting resistance $P_s$ in such a case can not be obtained, the area moment [$\Sigma(\Delta A \times Y_{ci})$] is calculated instead of the torque. Measured torque fluctuation is shown in Fig.14(b), which is drawn on the electromagnetic oscillograph through the strain gauge stuck on the hob arbor.

This also is almost similar to Fig.(a), but in order that (a) may agree precisely with (b), values of $P_s$ to multiply on the area moment of Fig.(a) must be varied between 228 and 347 $Kg/mm^2$. Thus, the calculated torque fluctuation will give a clue to the vibration analysis in the hobbing.

## 4. Conclusions

The hobbing mechanism in the unfinished tooth space was numerically analyzed in this paper.

A summary of the results is as follows:

(1) A new calculating method was proposed, which bases on the fact that many line segments imagined in the tooth space are gradually shortened by cutting with every hob tooth

(2) The cutting zone, thickness, length and the entering angle can be exactly calculated in the spur gear hobbing and the helical one in this way.

(3) Examples of calculation under various conditions are shown and it is confirmed that these examples agree well with the practically hobbed results.

(4) This method can be applied to the analyses of the tooth wear, the torque fluctuation, the design of special-shaped hob and so on.

## References

(1) Moncrieff, A.D., Tool Engr., 26 (1951) 25.

(2) Ainoura, M. et al., JSME Preprint (in Japanese), No.134 (1960 - 4), 65.

(3) Ainoura, M., Kikaino-Kenkyu (in Japanese), 14 - 8 (1962 - 8), 985.

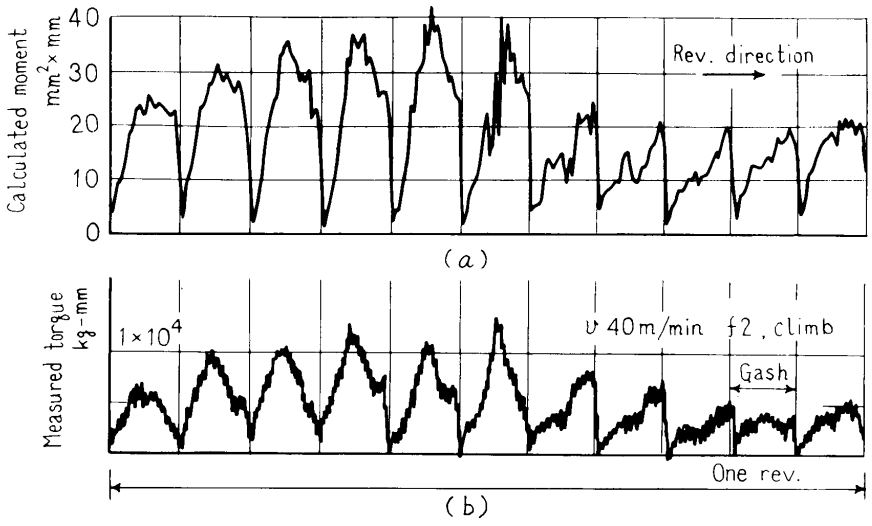


Fig.14 Calculated and measured cutting torque